Experimental and numerical investigation of a transcritical CO2 air/water reversible heat pump: analysis of domestic hot water production

Giacomo Tosato[(a)], Paolo Artuso[(a)], Silvia Minetto[(a)], Antonio Rossetti[(a)], Yosr Allouche[(b)], Krzysztof Banasiak[(c)]

[(a)] National Research Council, Construction Technologies Institute,
Corso Stati Uniti 4 – 35127 Padova (Italy), artuso@itc.cnr.it
[(b)] NTNU Norwegian University of Science and Technology,
Trondheim, 7491, Norway 2
[(c)] SINTEF Energy Research, Trondheim, 7465, Norway

ABSTRACT

As a natural refrigerant, carbon dioxide is safe, economic and environmentally sustainable and can be successfully utilized in heat pump and refrigeration systems operating according to transcritical cycles. This paper describes the development of a CO2 air/water reversible heat pump, specifically investigating the domestic hot water (DHW) production operating mode. A dynamic model of the heat pump is developed with the software Simcenter Amesim. After validation against experimental data, the numerical model is utilized to predict the performance of the heat pump to a varying hot water demand, evaporator air inlet conditions and high pressure value, leading to the discussion of the optimal control strategy.

Keywords: Transcritical heat pump, Carbon Dioxide, Numerical model, COP, DHW, Energy Efficiency.

1. INTRODUCTION

Compared to the other commercially available refrigerants, CO_2 (R744) offers negligible GWP (1/0) while being non-toxic, not-flammable and future-proof safe for human beings and for the environment. In the last fifteen years, several theoretical and experimental studies have been conducted on transcritical CO_2 systems (Neksa 2002, Ma et al. 2013) which demonstrated CO_2 heat pumps for DHW to be environmentally friendly and energy efficient. However, as the HVAC&R sector is undergoing a revolution caused by phase out and phase down of high GWP fluids, CO_2 has been progressively considered also for space or process heating and cooling. The EU funded project MultiPACK has the main goal of installing in the field integrated units for heating, cooling and DHW production, based on CO_2 and adopting two-phase ejectors to improve efficiency at high gas cooler outlet temperature. In this paper the circuit, which is detailed in Hafner et al, 2020, is simplified to the mere DHW functionality and paper a dynamic numerical model is developed using the software Simcenter Amesim v.17. Thanks to experimental data collected during a MultiPACK pre-commissioning test campaign, the numerical model is validated in both dynamic and steady state conditions and it is used to simulate a typical operation of the heat pump coupled to a water storage tank.

2. THE NUMERICAL MODEL OF THE MULTIPACK HEAT PUMP IN DHW OPERATIONS

2.1. The experimental apparatus

The operating scheme of the heat pump and water circuit are reported in Figure 1, while the geometric dimensions of its main components are summarised in Table 1. During operation, the refrigerant leaves the low-pressure receiver (6) in the state of saturated vapour and enters the low-pressure side of the internal heat exchanger (3).The compression of the refrigerant to the supercritical state is achieved with the parallel of two semi-hermetic compressors. The compressor (1a) is inverter controlled and it is controlled on water outlet temperature, while compressor (1b) operates at fixed speed. After the compression, the refrigerant in

supercritical state flows in a single-pass brazed plate gas-cooler (2) where rejects heat to the water before entering the high-pressure side of the internal heat exchanger where it is further cooled down. The refrigerant is then expanded to the evaporation pressure by a back-pressure valve (4), whose cross section is modulated by a PI controller to maintain the design high-pressure value $p_{HP}^{set-point}$.

Table 1. Dimensions of the heat pump main component

|	
Compressors (1)	Two reciprocating, semi-hermetic, single stage parallel compressors. Displacement volume 180.6 cm^3 (1a) and 205.0 cm^3 (1b).
Gas cooler (2)	Counter flow, single pass brazed plate heat exchanger. Heat transfer area of 8.90 m^2
Internal heat exchanger (3)	Counter flow, tube-in-tube type heat exchanger. Heat transfer area: Low pressure side 0.20 m^2, high pressure side 0.22 m^2
Expansion valve (4)	Electrically operated step motor valve. Maximum opening diameter 4.8 mm
Evaporator (5)	Finned coil heat exchanger, external area 491 m^2
Low pressure receiver (6)	Carbon steel receiver. Internal volume of 0.155 m^3

(a)   (b)
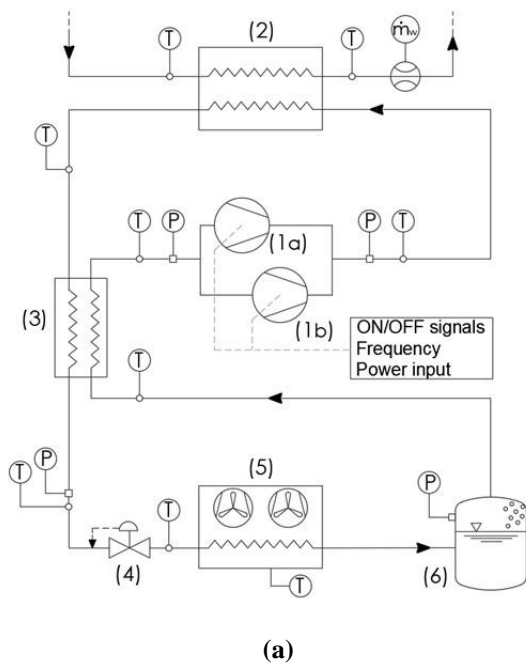
Figure 1: Transcritical heat pump (a) Schematic (b) Experimental apparatus

After the expansion, the two-phase mixture is evaporated to the state of saturated vapour in a finned coil evaporator (5) which is equipped with 4 EC axial fans, before flowing back in the low-pressure receiver. In the water circuit, the water mass flow rate flowing in the brazed-plate gas cooler is modulated by a variable speed pump to maintain the set point outlet temperature. On the other hand, the inlet air of the evaporator is taken from the surrounding environment where the finned coil is located. Experimental data was collected using 8 T-type thermocouples (accuracy ±0.2 K), 4 pressure transducers (accuracy of ±0.24 bar) and an electromagnetic flowmeter (accuracy of 1 % on the read value with velocity between 0.4 and 10 ms^{-1}), installed on the experimental apparatus according to Figure 1. In particular, the value of the evaporator inlet temperature (and thus pressure) is measured before the distributor of the finned-coil, so that the pressure drop in the evaporator comprehends the localized loss in the distributor.

2.2. The dynamic numerical model

The numerical model of the heat pump was developed with the software Simcenter Amesim v.17: the libraries of the software are composed of basic elements designed to model the transient behaviour of the internal and external flow, i.e. refrigerant, water and ambient air. The thermodynamic properties of carbon dioxide are evaluated with the Modified Benedict Webb Rubin formulation and the presence of oil in the refrigerant flow

was neglected. The water is assumed to be pure and its thermodynamic properties are calculated with Bode's formulation while the air is considered as a mixture composed by a combination of pure fluids which are weighted by its concentrations. The basic elements are coupled to develop the sub-model of the main components of the system (compressor, gas-cooler, internal heat exchanger, expansion valve, evaporator, low-pressure receiver and control system), which are connected to form the complete numerical model of the heat pump, with the same modelling approach already discussed in detail in Artuso et al. 2020 . The system includes both mass flow devices (compressors, expansion device) and energy flow devices (evaporator, gas-cooler, internal heat exchanger): as the dynamics of the mass flow devices are generally an order of magnitude faster than those of the heat exchangers, according to Rasmussen et al. (2005), the compressor and expansion device are both considered static components and modelled with steady-state empirical correlations. The semi-hermetic compressors are modelled as fixed-displacement compressors and the value of volumetric efficiency (η_V) and compression efficiency (η_C), necessary to evaluate the developed mass flowrate ($\dot{m}_V = \rho_{suc} V_d \frac{n}{60} \eta_V$) and electric power draw ($P_{el} = \dot{m}_V \Delta h_{is} / \eta_C$), are supplied by the compressors' manufacturer. The back-pressure expansion valve is modelled as a variable cross section expansion device, where the opening degree is adjusted by a PI controller to maintain the set-point high pressure. The low-pressure receiver is modelled as an adiabatic volume with a constant cross-section area and the operating pressure is constant in the entire volume. The modelling of the heat exchangers, which are characterized by a more complex nature, is conceived with a discretization of the device into smaller volumes, each treated with a lumped parameters approach. The gas-cooler numerical model is obtained with the assumption of homogeneous distribution of both refrigerant and water flow. With this assumption, the flow is modelled using a single equivalent pipe as reported in Figure 2. The heat transfer area A_{HX} and the hydraulic diameter ($D_h = 2b_p / \phi_p$) are determined by the geometric dimensions of the heat exchanger while the cross sectional area of the equivalent pipe is set equal to the total cross-sectional area of the heat exchanger ($A_{c,tot-gc} = N_{canal} A_{c,1canal}$). The corresponding length of the pipe is then defined according to Eq.1:

$$L_{pipe} = {A_{HX} D_h}\big/{4 A_{c,tot}} \qquad \text{Eq. (1)}$$

The equivalent pipe is then discretized into N_{disc} elements and the length of the pipe and heat transfer area are equally distributed in each element. The finned coil evaporator and the regenerative heat exchanger are modelled with the same approach described for the gas cooler.
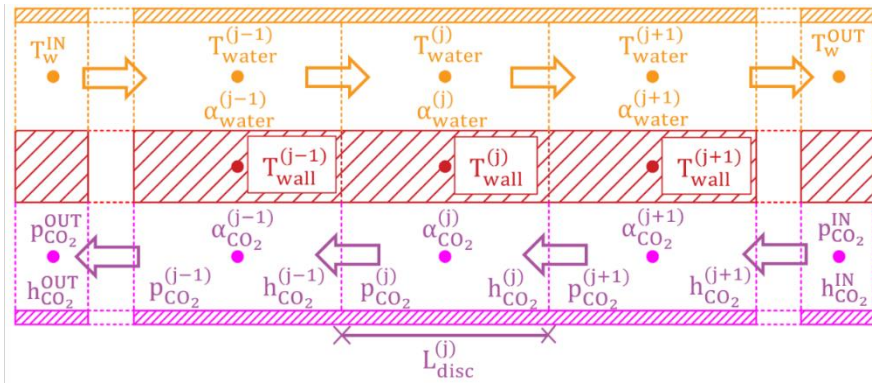

Figure 2: Schematic of the numerical model of the gas-cooler

In the evaporator, the hydraulic diameter of the equivalent tube is equal to the internal diameter of a single tube and the cross-sectional area is equivalent to the total cross sectional area considering all the 44 circuits of the heat exchanger. For the air side, the fans of the heat exchanger are considered to operate continuously and developing a constant mass flow rate; the presence of moisture on the inlet air is considered; however the performance degradation due to the presence of frost which will most likely occur for below 0 °C evaporation temperatures is neglected, as well as the defrost operation. The refrigerant pressure drop in the sub-models is evaluated with the Mac-Adams correlation while the water and air pressure drop is neglected, the heat transfer coefficients of the water and refrigerant flowing in the heat exchange devices are evaluated using empirical correlations which are available in literature. A sensitivity analysis on the heat exchangers sub-models determined that the evaporator and the regenerative heat exchanger had to be discretized into 10 elements to

obtain a satisfactory accuracy on the numerical solution. On the other hand, due to the high variability of the thermal properties of supercritical CO_2, the gas-cooler had to be discretized into a minimum of 25 elements. A total of 30 elements were chosen, as a compromise between accuracy of numerical solution and solver convergence time. The input to the numerical model are the geometric dimensions of the main components, the state of the water at the inlet of the gas-cooler (T_{water}^{IN}, p_{water}^{IN}, $\dot{m}_{water}$) and the state of the air at the inlet of the finned-coil evaporator (T_{air}^{IN}, φ_{air}^{IN}, $\dot{m}_{air}$). The model provides as output the state of the refrigerant in the heat pump, the heat flow rate ($\dot{Q}_{gc}$, $\dot{Q}_{eva}$, $\dot{Q}_{IHX}$) and the state of the water and air at the gas-cooler/evaporator outlet.

2.3.   Numerical model validation

The validation of the numerical model was provided in both steady-state and transient operation. For the steady-state operation, the model demonstrated to be in good agreement with the experimental data (see Table 2 and Figure 3). The heat pump boundary conditions (i.e. input to the numerical model) are defined by $\dot{m}_{air}^{IN}=$ 25.2 kgs^{-1}, $T_{air}^{IN} = 8.7$ °C, $\varphi_{air}^{IN}= 67$ % and $\dot{m}_w= 2$ kgs^{-1}, $T_w^{IN} = 23.9$ °C for the air side and water side respectively.

Table 2- Validation of the numerical model operating in steady-state condition

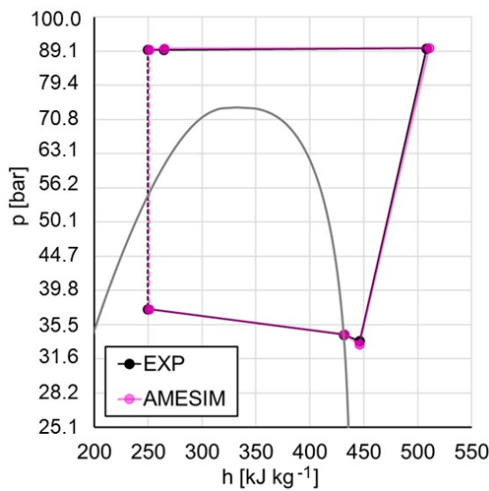| SIMULATION OUTPUT			
$\dot{Q}_{gc}^{EXP}$=169.3 kW	$T_{w,OUT}^{EXP} = 44.2$ °C	$\dot{Q}_{IHX}^{EXP}=$ 9.6 kW	$\bar{p}_{LPR}^{EXP} = 34.4$ bar
$\dot{Q}_{gc}^{AMESIM}$=165.6 kW	$T_{w,OUT}^{AMESIM} = 43.2$ °C	$\dot{Q}_{IHX}^{AMESIM}=$ 10.1 kW	$\bar{p}_{LPR}^{AMESIM} = 34.5$ bar
(+2.2%)	(-1 K)	(+5.2%)	(+0.1 bar)

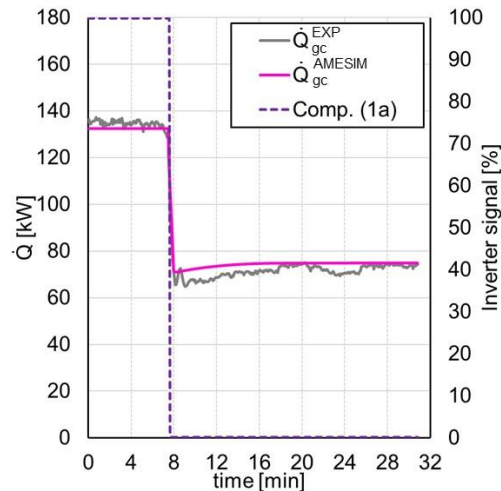**Figure 3: Operation of the heat pump in p-h diagram, EXP vs. AMESIM**

Figure 4: Trend of gas-cooler heat flow rate as a function of time, EXP vs. AMESIM

The numerical validation in transient conditions was obtained by suddenly shutting down the compressor (1a) (7.5 min) after the system had previously reached steady state operating condition. Figure 4 reports the trend of $\dot{Q}_{gc}$ as a function of time during the steady state condition prior to the compressor shutdown, the transient evolution (7.5 min-24.5 min) and the successive steady state operation (24.5 min-30 min). The model was found to be in good agreement with the experimental data, as the mean percentage variation between simulated and experimental value of $\dot{Q}_{gc}$ was found to be equal to +1.75%, +5.03% and +1.95% for the three zones respectively.

3. SIMULATION OF THE HEAT PUMP DURING OPERATION

After validation, the numerical model was utilized to simulate the operation of the system coupled with a stratified water tank storage. Since in this paper the water tank storage is not modelled, the return water temperature profile, i.e. T_{water}^{IN}, was taken from experimental data collected in a previous study (Tosato et al. 2019) and reported in Figure 5 as a function of the reduced volume V* which is defined as the ratio between the actual volume removed by the circulating pump and the total volume of the storage. In the numerical model, the simulation of the circulating pump is performed with a constant mass source, modulated by a PI controller, in order to satisfy the constrain on the required value of water temperature at the gas-cooler outlet.
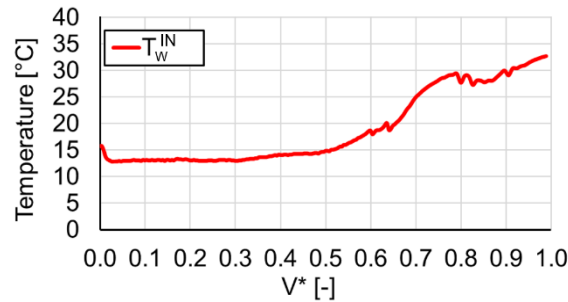

Figure 5- Trend of the return water inlet temperature as a function of the non-dimensional volume

The operation of the heat pump was simulated for different values of water set-point temperature and for different conditions of the air at the evaporator inlet (T_{air}^{IN}, φ_{air}^{IN}) while the value of high pressure was kept constant at 105 bar. For the state of the air at the evaporator inlet, the mean temperature and relative humidity of the heating months (October-April) of Treviso, where the experimental apparatus is located, were chosen. As for the water set-point temperature, it was varied from 60 °C to 80 °C. For the control strategy of the heat pump, it was chosen to turn off the system once a total of 300 kWh had been provided at the water tank storage. Figure 6 then reports the trend of COP as a function of the supply water set point temperature and for different mean ambient conditions of Treviso during the typical heating months.
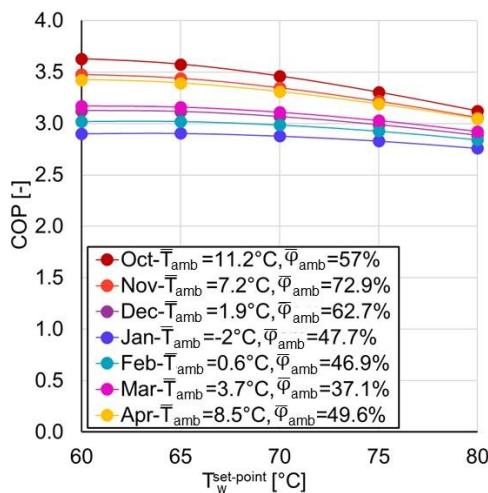

Figure 6- Trend of COP as a function of the water set point temperature and external environment conditions
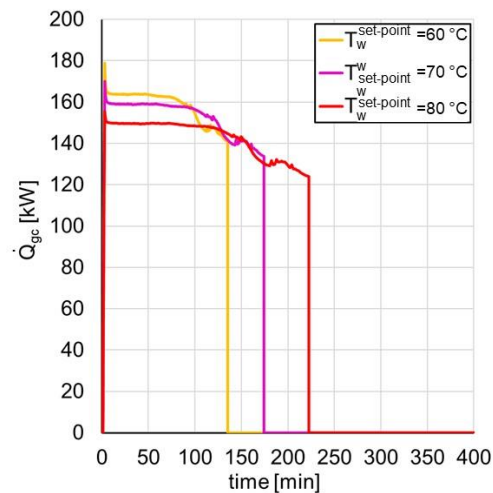

Figure 7- Trend of gas-cooler heat flow rate for different values of water set point temperature during the month of March

On the other hand, in Figure 7 it is possible to observe the trend of gas-cooler heat flow rate during operation of the heat pump for different values of the supply water set-point temperatures. In this case, the ambient conditions of March in Treviso were chosen, as they are the closest ones to the mean conditions of the entire heating seasons. The set point temperature of 60 °C presents the highest value of heat flow rate, due to a higher value of mass flow rate that must be elaborated, leading consequently to an higher COP and a reduced on-stage of the heat pump, as the 300 kWh are stored more quickly.

4. CONCLUSIONS AND FUTURE WORK

This paper provides a numerical model of an air to water heat pump which was built up and fully instrumented. The numerical model was conceived with the commercial software Simcenter Amesim v.17 and validated in both dynamic and steady state conditions. The numerical model demonstrated good agreement with the experimental data collected during steady state operation of the heat pump as the mean percentage variation between simulated and experimental value of gas-cooler heat flow rate was found to be equal to +2.2%, +1.95% and +1.75% respectively for the three different operating conditions. The model was then utilized to simulate the operation of the system when coupled to a stratified water tank storage and addressed that when operating with a set-point heating temperature of 60 °C, the gas-cooler provided the highest value of heat flow rate, due to a higher value of mass flow rate which had to be elaborated, leading consequently to a higher COP. The development of a reliable numerical model represents the first step in the discussion of the optimum control strategy of the heat pump during operation. Future work will comprehend the coupling of the numerical model presented in this paper with the numerical model of an actual stratified water tank storage, in order to consider the interactions between the two systems and discuss the control strategy and thermal performance of the complete system.

NOMENCLATURE

$A_{c,tot}$	Total cross sectional area (mm^2)	$A_{c,1canal}$	Cross sectional area of a single canal (mm^2)
A_{HX}	Heat transfer area (m^2)	b_p	Distance between plates (mm)
D_h	Hydraulic diameter (mm)	ϕ_p	Surface enlargment factor (-)
φ	Relative humidity	L_{pipe}	Length of the equivalent pipe (m)
L_{disc}	Length of the discretized pipe (m)	$\dot{m}$	Mass flow rate (kg s^{-1})
N_{disc}	Number of discretizations (-)	N_{canals}	Number of canals (-)
T	Temperature (°C)	α	Heat transfer coefficient (Wm^{-2}K^{-1})

REFERENCES

Artuso P., Marinetti S., Minetto S., Del Col D., Rossetti A., 2020, Modelling the performance of a new cooling unit for refrigerated transport using carbon dioxide as the refrigerant, International Journal of Refrigeration, vol. 115: p.158-171.

Ma, Y.T.; Liu, Z.Y.; Tian, H., 2013, A review of transcritical carbon dioxide heat pump and refrigeration cycles. Energy 55, 156–172

Hafner, 2020, Development of CO2 refrigeration technology between 1995 and 2020, 14th Gustav Lorentzen Conference, Kyoto, Japan, 6th- 9th December, 2020

Neksa, P., 2002, CO$_2$ heat pump systems, International Journal of Refrigeration, vol. 25: p. 421-427.

Rasmussen B.P., 2005. Dynamic modelling and advanced control of air conditioning and refrigeration systems, Ph.D. thesis, University of Illinois at Urbana-Champaign, USA

Tosato G., Girotto S., Minetto S., Rossetti A., Marinetti S, 2019, An integrated CO$_2$ unit for heating, cooling and DHW installed in a hotel. Data from the filed. 37th UIT Heat Transfer Conference. Padova, 24-26 June 2019